

Evaluation of dual-energy and perfusion CT parameters for diagnosing solitary pulmonary nodules

Beilin Zhu | Shuo Zheng | Tao Jiang  | Bin Hu

Beijing Chaoyang Hospital affiliated to Capital Medical University, Beijing, China

Correspondence

Tao Jiang, Department of Radiology, Beijing Chaoyang Hospital affiliated to Capital Medical University, Beijing, 100020, China.
Email: dr_jiangt@163.com

Bin Hu, Department of thoracic surgery, Beijing Chaoyang Hospital affiliated to Capital Medical University, Beijing 100020, China.
Email: hubin705@aliyun.com

Abstract

Background: To evaluate the correlation and accuracy of dual-energy CT (DECT) (70/Sn150) and low-dose volume perfusion CT (VPCT) parameters for the diagnosis of solitary pulmonary nodules (SPN).

Methods: A total of 15 patients with benign SPN (mean age 56 ± 7 years) and 34 patients with malignant SPN and clinical indication for surgery (mean age 58 ± 6 years) were enrolled from July 2017 to September 2019 at a single institution. All the patients underwent low-dose VPCT with a scan volume of 114 mm on the z-axis and a venous phase enhancement DECT (70/150 Sn) scan just before surgery on the same day. All CT findings were studied in comparison with the pathological results after surgery. Perfusion and dual-energy CT parameters such as blood flow (BF), blood volume (BV), mean transit time (MTT), flow extraction product (FED), pulmonary nodule enhancement peak (PPnod) and iodine concentration (IC) were evaluated as well as *t*-test, chi-square test, Pearson correlation analysis, and ROC curve analysis to determine the significance of study parameters.

Results: The effective radiation dosage of the VPCT and DECT scans were 4.67 ± 0.26 mSv and 0.32 ± 0.10 mSv, respectively. Significant correlations were found between iodine concentration from DECT and VPCT parameters ($r = 0.376$ – 0.533 , $p < 0.05$). The sensitivity and specificity of IC to differentiate the SPN were 86.67% and 72.73%, which was slightly lower than that of BV (94.44%, 73.33%), FED (88.89%, 80.00%) and PPnod (94.44%, 80.00%).

Conclusions: VPCT scans have low radiation dosage achieved by shortening the z-axis scan range for assessment of SPN. IC from DECT is significantly correlated with VPCT parameters, and VPCT parameters have better diagnostic performance for SPN than DECT parameters.

KEYWORDS

dual-energy, perfusion, radiation dosage, solitary pulmonary nodules

INTRODUCTION

Solitary pulmonary nodules (SPN) are a common disease of the lung, which are caused by varied factors including tumors, inflammation, infection, blood vessels, and congenital abnormalities. SPN are characterized by rounded or irregular opacity, and are well or poorly defined, measuring up to 3 cm in diameter.¹ According to their attenuation, SPN can be classified as solid or subsolid, the latter further

divided into pure ground-glass nodules (pGGN) and part solid nodules, with part-solid nodules having both ground-glass and solid components.² Studies have indicated that the probability a given nodule is malignant increases according to its size, ranging from 0%–1% for nodules <5 mm, 6%–28% for those 5–10 mm, and from 64%–82% for nodules >20 mm.^{2,3} According to the eighth edition of the Lung Cancer Stage Classification,⁴ the 5-year survival rates of categories IA1, IA2, IA3 and IB are 90%, 85%, 80%, and

73%, respectively. The “downside” of follow-up studies utilizing low-dose screening computed tomography (CT) includes unnecessary patient anxiety, increased radiation burden, among others,⁵ emphasizing the importance of early diagnosis. High resolution chest CT is considered to be the standard technique for evaluating morphological characteristics. However, differentiating malignant from benign SPN is always a challenge for the radiologist when only traditional CT data are available, as there is a huge overlap between malignant and benign morphological findings.⁶

The formation of new blood vessels within tumors is essential for tumor growth and metastasis. The development of new vessels leads to physiological changes, specifically increased perfusion, blood volume, and capillary permeability.⁷ Volume perfusion CT (VPCT) enables quantitative analysis of tumor tissue by measuring flow and concentration of iodinated contrast medium within blood vessels and tissue during a specified time period, which generates time density curves (TDC). The parameters of VPCT are regarded as a noninvasive approach to evaluate tumor angiogenesis.^{8,9} Dual-energy CT (DECT) is capable of generating material decomposition images, which can be used to measure the iodine component of SPN on iodine-enhanced images, which is considered to be equivalent to the actual value of enhancement. With DECT, patient safety is increased by reducing the amount of required contrast agent and by omitting a true unenhanced CT.¹⁰

In our study, the two modalities are explored in order to assess their diagnostic power in recognizing malignant SPN, and the correlation between parameters obtained from both techniques.

METHODS

Patients

The local institutional review committee approved the study, and informed consent was obtained from all patients before CT examinations. A total of 51 patients met the inclusion criteria, and 49 patients with single SPN who had a clinical indication for surgery were finally enrolled from July 2017 to September 2019 at a single institution. Two patients had to be excluded due to motion artifacts and beam-hardening artifacts on the CT images.

Clinical information such as age, gender, nodule sizes, morphology, hospital stay duration, clinical symptoms, smoking status, and nodule location was compared between patients with benign and malignant SPN (Table 1). Morphological characteristics on a chest CT scan suggestive of malignancy included spiculated margins, vessel convergence, and pleural retraction.⁶ The clinical symptoms (9/49) mainly included cough and sputum, chest tightness, and chest pain.

All patients were diagnosed with SPN by noncontrast enhanced chest CT and enrolled in the study based on the following criteria: (1) no previous history of other systemic malignancies; (2) no preoperative radiotherapy, chemotherapy,

targeted therapy, or immunotherapy; (3) presence of solitary pulmonary nodules with no calcification and no clear fat composition; (4) no recent history of pneumonia or immunodeficiency; and (5) no contraindications to contrast medium administration.

VPCT and DECT imaging protocol

All scans were performed with a 192-slice third-generation dual-source CT scanner (SOMATOM Force, Siemens Healthineers). The protocol consisted of a nonenhanced chest CT (NECT) for localizing the SPN (90 kV, 55 mA). Subsequently, a scan volume of 114 mm on the z-axis was placed to cover the pulmonary nodule, followed by a volume perfusion CT of the lesion using 70 kv and 80 mA. Additional scan parameters were 0.25 s rotation time and 48×1.2 mm section collimation. Twenty-one scans were performed every 1.5 s commencing 4 s after the contrast material injection. The short delay of 4 s was chosen to ensure the acquisition of at least one nonenhanced dataset, as previously shown, leading to a total examination time of 34.85 s. In each patient, 50 ml iodinated contrast was injected into an antecubital vein at a flow rate of 5 ml/s followed by 40 ml saline solution at the same flow rate. After acquiring the VPCT data, take a breath, and then hold breath again, a DECT scan was acquired (CARE Dose 4D,70/Sn150kV, Acq. 192×0.6 mm, pitch 0.55, rotation time 0.25 s, scan time 1.05 s). If a patient was unable to hold their breath for this duration, they were instructed to breath as shallow as possible. Before the examination, each patient had repeated communication and breathing training. As none of the patients had basic pulmonary diseases, the cooperation of the 49 patients included in the study was satisfactory.

Perfusion CT images were reconstructed with a section thickness of 5 mm (increment, 3 mm) by using a body convolution kernel (Br36), and TDC images were reconstructed with a section thickness of 1 mm (increment, 0.7 mm) by using a convolution kernel (Bl64).

A radiation dose parameter, dose-length product (DLP), was taken from the patient protocol and recorded in the CT protocol, in order to calculate the effective dose (ED). $ED = DLP \times K$, in units of mSv, and K was the conversion factor ($K = 0.014$ mSv/mGy·cm).

VPCT and DECT data reconstruction

Quantitative VPCT and DECT data were evaluated with commercial software (Syngo Volume Perfusion CT Body and CT dual-energy, VB10, Siemens Healthcare), which is based on deconvolution. First, motion correction was applied to each VPCT examination. 4D noise reduction was then applied to improve the signal to noise ratio for SPN. Regions of interest (ROI) were placed in the thoracic aorta for measuring the arterial input function and a TDC was obtained. Next, the soft tissue region of the pulmonary

TABLE 1 Clinical information

Characteristics	Pathology		t/χ^2	p -value	
	Benign	Malignant			
Age	56.33 ± 7.41	58.47 ± 6.49	-1.017	0.314	
Hospital stays	12.47 ± 7.43	12.58 ± 4.26	-0.053	0.958	
Size (mm)	12.27 ± 5.66	15.64 ± 6.08	-1.818	0.076	
Gender	Male	10 (66.7%)	8 (23.5%)	8.334	0.004 ^a
	Female	5 (33.3%)	26 (76.5%)		
Clinical symptoms	No	12 (80.0%)	28 (82.3%)	0.038	0.845
	Yes	3 (20.0%)	6 (17.7%)		
Smoking	No	6 (40.0%)	28 (82.3%)	8.789	0.003 ^a
	Yes	9 (60.0%)	6 (17.7%)		
Nodule location	Upper lobe	7 (46.7%)	21 (61.8%)	2.762	0.251
	Middle lobe	4 (26.7%)	3 (8.8%)		
	Inferior lobe	4 (26.7%)	10 (29.4%)		
Morphology	Spiculated margins	1 (6.7%)	19 (55.9%)	10.44	0.001 ^a
	Vessel convergence	5 (33.3%)	20 (58.8%)		
	Pleural retraction	4 (26.7%)	22 (64.7%)		

^aResults between the two groups were significantly different, $p < 0.05$.

nodule was selected as another ROI, avoiding the visible blood vessel and liquefaction necrosis area. Through this ROI positioning, the software calculated the following CT perfusion parameters automatically: blood volume (BV) (ml/100 g), blood flow (BF) (ml/100 g/min), mean transit time (MTT) (s), time to peak (TTP) (s), Flow extraction product (FED) (ml/100 g/min), pulmonary nodule enhancement peak (PPnod) (Hu), aorta enhancement peak (PPao) (Hu) and the ratio of PPnod to PPao (PPnod/PPao).

For DECT parameter acquisition, iodine concentration (IC) of the nodule was measured on the iodine-based image by using an operator-defined ROI around the entire nodule. In order to minimize variation between patients, the nodule IC was normalized to IC in the aorta to derive a normalized iodine concentration (NIC): $NIC = IC_{tumor}/IC_{aorta}$.

Dual-energy CT outcome parameters included iodine concentration (IC), normalized iodine concentration (NIC) and slope of the spectral HU curve ($\lambda = [CT_{40KeV} - CT_{100KeV}]/60$).

Statistical analysis

Data analysis was performed using SPSS 21.0 (IBM SPSS). All data were expressed as mean ± standard variation. Significant significance was set at p less than 0.05. Pearson correlation coefficients were used to assess relationships between the perfusion and DECT parameters. Both t - and Chi-square tests were used to compare values of diameters, volume, VPCT parameters, and DECT parameters between malignant and benign SPN. The pathological examination was used as the golden standard. The ability of VPCT and DECT values to distinguish between malignant and benign

SPN was assessed with receiver operating characteristic (ROC) analyses. The accuracy, sensitivity, and specificity of each quantitative parameter in the diagnosis of SPN were calculated.

RESULTS

Patients

The benign SPN size was 12.27 ± 5.66 mm, and the size of malignant SPN was 15.64 ± 6.08 mm, ranging from 6 to 29 mm for all SPN included. Fifteen patients with benign SPN (mean age 56 ± 7 years) and 34 patients with malignant SPN (mean age 58 ± 6 years) were enrolled. Clinical information is shown in Table 1. Twenty-eight nodules were located in the upper lobe of the lung, seven were located in the right lung middle lobe, and 14 were located in the lower lobe of the lung.

The pathological type of 33 solid nodules were as follows: 18 malignant nodules (16 nodules of invasive adenocarcinoma, two nodules of squamous cell lung cancer), 15 benign nodules (five nodules of hamartoma, four nodules of tuberculoma, two nodules of intrapulmonary lymph node, four nodules of other pathology). The pathological type of 16 sub-solid nodules were: 11 nodules of adenocarcinoma in situ (AIS), two nodules of microinvasive adenocarcinoma (MIA), and three nodules of invasive adenocarcinoma (IA).

The DECT DLP was 23 ± 8 mGy-cm. The total VPCT DLP was 338 ± 8 mGy-cm (including a 64 mGy-cm NECT dose and a 274 mGy-cm VPCT dose). The ED of the VPCT and DECT scans were 4.67 ± 0.26 mSv and 0.32 ± 0.10 mSv, respectively.

TABLE 2 VPCT and DECT quantitative parameters of benign and malignant SPN

Parameter	Accuracy (AUC)	Standard error (SE)	<i>p</i> -value	Cutoff value	Sensitivity (%)	Specificity (%)
BV	0.859	0.0712	<0.0001 ^a	>4.13	94.44	73.33
BF	0.793	0.0852	0.0006 ^a	>69.32	88.89	66.67
MTT	0.602	0.0936	0.2763	>4.63	44.44	93.33
FED	0.863	0.0652	<0.0001 ^a	>23.55	88.89	80.00
TTP	0.620	0.104	0.2472	≤19.96	72.22	60.00
PPnod	0.865	0.0761	<0.0001 ^a	>44	94.44	80.00
PPnod/PPaor	0.756	0.0926	0.0058 ^a	>5.48	72.22	86.67
IC	0.742	0.107	0.0230 ^a	>1	86.67	72.73
NIC	0.594	0.126	0.4569	>0.41	66.67	63.64
λ	0.648	0.122	0.2245	≤3.82	93.33	45.45

Abbreviations: BF, blood flow; BV, blood volume; FED, flow extraction product; IC, iodine concentrate; MTT, mean transit time; NIC, normalized iodine concentration; PPnod, Pulmonary nodule enhancement peak; TTP, time to peak; λ, slope of the spectral HU curve.

^aResults between the two groups were significantly different, *p* < 0.05.

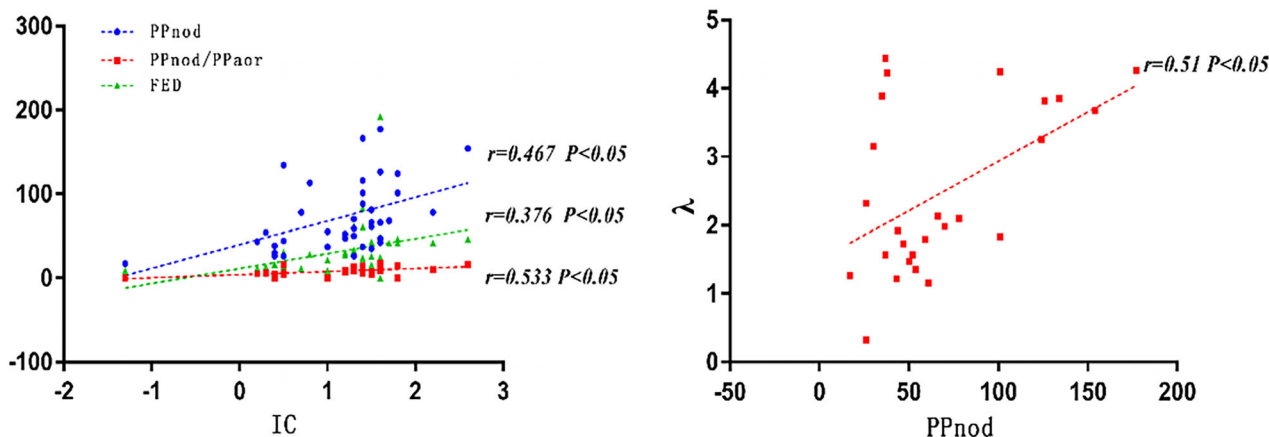


FIGURE 1 Correlation between DECT and VPCT parameters

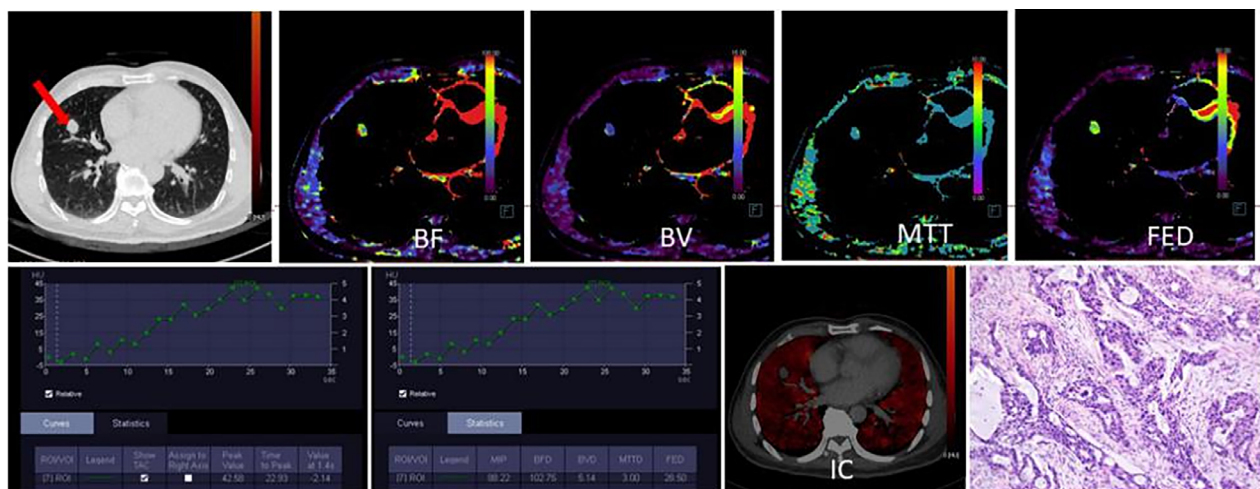


FIGURE 2 VPCT and DECT quantitative analysis of invasive adenocarcinoma in a 72-year-old male with a solid nodule in the right middle lobe. Time density curves (TDC) had an obvious increase in nodular HU value and a steeper slope. Axial functional maps show BF, BV, MTT, FED, IC; value of IC is 1.2 mg/ml. The case was confirmed as invasive micropapillary adenocarcinoma by pathology

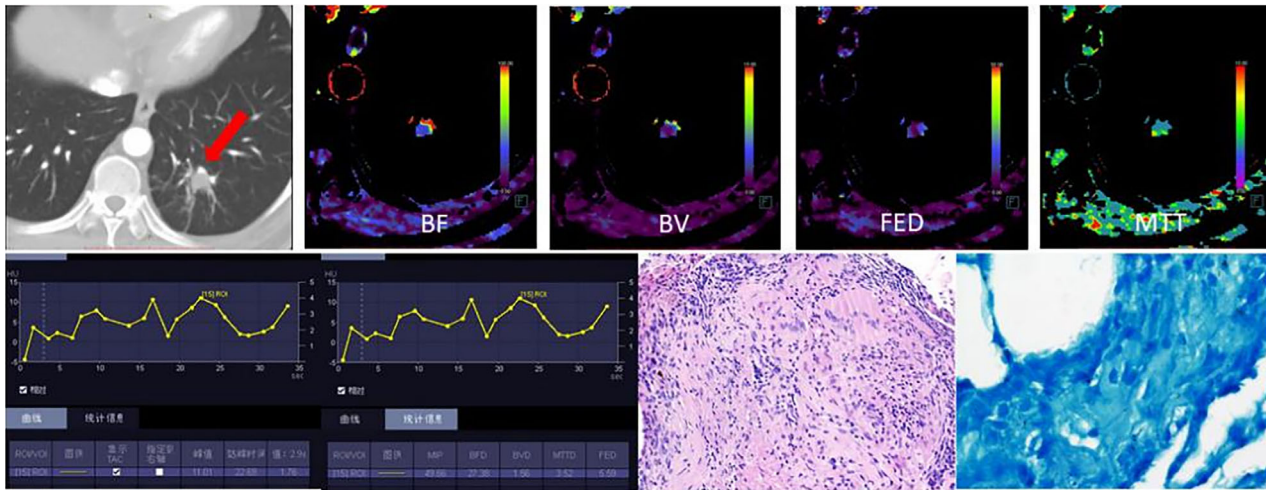


FIGURE 3 VPCT quantitative analysis of tuberculoma in a 57-year-old male with a solid nodule in the left lower lobe. Time density curves (TDC) show that enhancement of the nodule is relatively low. The axial functional maps show BF, BV, FED, MTT. The case was confirmed as tuberculoma by pathology with a picture of granulomas and positive acid-fast stain

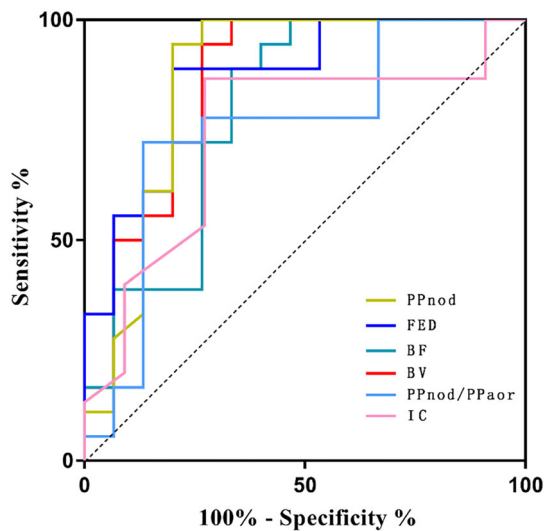


FIGURE 4 ROC curve of the quantitative parameters

Perfusion CT and DECT quantitative analysis

Table 2 shows the VPCT and DECT quantitative parameters of benign and malignant SPN. Except for MTT, TTP, NIC, and λ , all other parameters (BV, BF, FED, PPnod, PPnod/PPao, and IC) showed significant differences ($p < 0.05$) between the benign SPN and malignant SPN.

Correlation results are shown in Figure 1. The IC of the nodules were significantly correlated with FED ($r = 0.376, p < 0.05$), PPnod ($r = 0.467, p < 0.05$) and PPnod/PPao ($r = 0.533, p < 0.05$). Examples of perfusion and iodine concentration parametric maps are shown in Figures 2 and 3.

ROC diagnostic implication

ROC curves were created, and the AUC was calculated for parameters that were significantly different between benign and malignant SPN (Table 2, Figure 4). BV, BF, FED, PPnod, PPnod/PPao from VPCT and IC from DECT showed strong ability to differentiate benign and malignant nodules with AUC values of 0.859, 0.793, 0.863, 0.865, 0.756, and 0.742, respectively. The diagnostic sensitivity and specificity values are summarized in Table 2. The sensitivity and specificity of IC in differentiating the SPN were 86.67% and 72.73%, which were slightly lower than that of BV (94.44%, 73.33%), FED (88.89%, 80.00%) and PPnod (94.44%, 80.00%).

DISCUSSION

Our study results showed that iodine parameters from DECT are significantly correlated with FED ($r = 0.376, p < 0.05$), PPnod ($r = 0.467, p < 0.05$) and PPnod/PPao ($r = 0.533, p < 0.05$) from VPCT. According to previous reports, DECT has been suggested to be a potential surrogate for perfusion CT in advanced hepatocellular carcinoma,¹¹ pancreatic cancer,¹² and colorectal cancers¹³ because of the correlation to perfusion CT and lower radiation dose. However, our study also showed that the sensitivity and specificity of IC from DECT were slightly lower than that of BV, FED and PPnod from VPCT.

VPCT is a technique for consecutive multislice scanning of the same section of a lesion after an intravenous bolus of iodine contrast agent to obtain the TDC of each pixel in the section. BF, BV, PPnod, and FED were closely correlated with microvascular density (MVD) measurement.^{14,15} Many

studies also have demonstrated that VPCT an important method to noninvasively evaluate tumor angiogenesis and help to distinguish malignant SPN from benign and inflammatory SPN, which is important for risk stratification, assessing disease progression, and monitoring therapeutic response.^{7,9,16–18} In our study, the total DLP of VPCT was 338 ± 8 mGy·cm (including a 64 mGy·cm NECT dose and a 274 mGy·cm VPCT dose). The radiation dose of perfusion CT is the key factor impeding its application. However, our protocol had a very low radiation dose that is lower than the mean effective dose for a standard chest CT (about 7 mSv) from the National Lung Screening Trial reports and similar to the previously published DLP of routine chest CT (411 mGy·cm),¹⁹ Furthermore, morphological information and quantitative parameters can be obtained simultaneously with VPCT. Research also shows that although the effective radiation dose of LDCT is about 1.5 mSv, the radiation will be increased when further examination such as diagnostic lung CT, PET/CT scan examination is required.⁵ The dose level is considered a low-dose CT, and the National Comprehensive Cancer Care Network guidelines have suggested an effective dose of ≤ 3 mSv for patients with a body mass index (BMI) ≤ 30 kg/m² and ≤ 5 mSv for patients with a BMI >30 kg/m².

For DECT, the three materials in the thorax most frequently analyzed are iodine, air, and soft tissue. A single contrast material-enhanced acquisition can supply both virtual nonenhanced images and contrast-enhanced CT data, which may obviate the additional acquisition of true non-enhanced CT scans.^{11,20} In the study by Reiter et al.,²¹ the size of pulmonary nodules ≤ 3 cm were evaluated by DECT. A total of 118 nodules were included, and the sensitivity and specificity of visual assessment of enhancement were 100% and 44%. Another study compared CT numbers on iodine-enhanced images to the degree of enhancement on real enhanced images and showed differences in sensitivity (92.0% vs. 72.0%), specificity (70.0% vs. 70.0%), and diagnostic accuracy (82.2% vs. 71.1%).²²

In our study, the PET/CT was performed in few patients and none of the patients received MRI. Thus, it was impossible to compare the accuracy of VPCT with MRI or PET/CT. According to a meta-analysis, the accuracy of diffusion weighted imaging (DWI) in differential diagnosis of malignant and benign pulmonary lesions was 91%, slightly lower than that of FDG-PET (94%), VPCT (93%), and dynamic contrast-enhanced MRI (94%).²³ Ruilong et al.²⁴ also conducted a meta-analysis of the diagnostic value of 18F-FDG-PET/CT for the assessment of SPN, which showed good diagnostic performance, producing 82% for sensitivity and 81% for specificity. However, in a survey conducted by Li et al.,²⁵ combined preoperative FDG-PET/CT diagnoses in 298 patients with suspected malignant lung nodules clinically was compared with the histopathological results, and the sensitivity, specificity, PPV, NPV, and accuracy were 80%, 38%, 87%, 28%, and 73%, respectively.

PET and dynamic contrast material-enhanced MRI can be used to assess tumor microcirculation, but these

techniques are not often used for this indication due to low spatial resolution, high cost, and complicated and time intensive procedures.⁹ These studies suggest that these non-invasive procedures have all become increasingly robust within the past decade. However, VPCT can provide not only morphological information but also information about tumor blood vessels noninvasively, and can quantify angiogenesis in lung cancer. VPCT generates excellent diagnostic value when compared to other noninvasive procedures, which may be helpful for guiding clinical treatment.⁷ Therefore, DECT is not considered as a good alternative to VPCT in the assessment of tumor hemodynamics in patients with SPN. Based on more clinical experience and studies, the application of dual-energy and perfusion techniques in the evaluation of thoracic diseases can be expanded by adjusting the scanning protocol and post-management techniques.

There are limitations to the study. First, the sample size of 49 was relatively small and histological subtypes were not evenly distributed. Considering the diversity of SPN pathological types and the difference of hemodynamics in different pathological conditions, the relatively small sample size of this investigation inevitably leads to selection bias. Therefore, further studies in various pathological conditions are required to evaluate the diagnostic value of the methods. Second, in our study, we did not examine histological parameters such as MVD, and further studies are strongly recommended.

In conclusion, DECT and VPCT have low radiation dosage by shortening the z-axis scan range for SPN. IC from DECT is significantly correlated with VPCT parameters, VPCT parameters have good diagnostic performance for SPN, which are more significant statistically than DECT parameters for diagnosing benign and malignant nodules.

ACKNOWLEDGMENTS

The authors would like to express their gratitude to EditSprings (<https://www.editsprings.com/>) for the expert linguistic services provided.

CONFLICT OF INTEREST

The authors declare that they have no competing interests.

DATA AVAILABILITY STATEMENT

The datasets used and/or analyzed during the current study are available from the corresponding author on reasonable request.

ORCID

Tao Jiang  <https://orcid.org/0000-0002-4011-346X>

REFERENCES

1. Hansell DM, Bankier AA, MacMahon H, McLoud TC, Müller NL, Remy J. Fleischner Society: glossary of terms for thoracic imaging. *Radiology*. 2008;246:697–722.
2. Rampinelli C, Calloni SF, Minotti M, Bellomi M. Spectrum of early lung cancer presentation in low-dose screening CT: a pictorial review. *Insights Imaging*. 2016;7:449–59.

3. MacMahon H, Austin JH, Gamsu G, Herold CJ, Jett JR, Naidich DP, et al. Guidelines for management of small pulmonary nodules detected on CT scans: a statement from the Fleischner Society. *Radiology*. 2005;237:395–400.
4. Detterbeck FC, Boffa DJ, Kim AW, Tanoue LT. The eighth edition lung cancer stage classification. *Chest*. 2017;151:193–203.
5. Bach PB, Mirkin JN, Oliver TK, Azzoli CG, Berry DA, Brawley OW, et al. Benefits and harms of CT screening for lung cancer: a systematic review. *JAMA*. 2012;307:2418–29.
6. Gould MK, Donington J, Lynch WR, Mazzone PJ, Midthun DE, Naidich DP, et al. Evaluation of individuals with pulmonary nodules: when is it lung cancer? Diagnosis and management of lung cancer, 3rd ed: American College of Chest Physicians evidence-based clinical practice guidelines. *Chest*. 2013;143(5 Suppl):e93S–e120S.
7. Miles KA. Tumour angiogenesis and its relation to contrast enhancement on computed tomography: a review. *Eur J Radiol*. 1999;30:198–205.
8. Li Y, Yang ZG, Chen TW, Yu JQ, Sun JY, Chen HJ. First-pass perfusion imaging of solitary pulmonary nodules with 64-detector row CT: comparison of perfusion parameters of malignant and benign lesions. *Br J Radiol*. 2010;83:785–90.
9. Sun Y, Yang M, Mao D, Lv F, Yin Y, Li M, et al. Low-dose volume perfusion computed tomography (VPCT) for diagnosis of solitary pulmonary nodules. *Eur J Radiol*. 2016;85:1208–18.
10. Goo HW, Goo JM. Dual-energy CT: new horizon in medical imaging. *Korean J Radiol*. 2017;18:555–69.
11. Mulé S, Pigneur F, Quelever R, Tenenhaus A, Baranes L, Richard P, et al. Can dual-energy CT replace perfusion CT for the functional evaluation of advanced hepatocellular carcinoma? *Eur Radiol*. 2018;28:1977–85.
12. Stiller W, Skornitzke S, Fritz F, Klauss M, Hansen J, Pahn G, et al. Correlation of quantitative dual-energy computed tomography iodine maps and abdominal computed tomography perfusion measurements: are single-acquisition dual-energy computed tomography iodine maps more than a reduced-dose surrogate of conventional computed tomography perfusion? *Invest Radiol*. 2015;50:703–8.
13. Kang HJ, Kim SH, Bae JS, Jeon SK, Han JK. Can quantitative iodine parameters on DECT replace perfusion CT parameters in colorectal cancers? *Eur Radiol*. 2018;28:4775–82.
14. Wang M, Li B, Sun H, Huang T, Zhang X, Jin K, et al. Correlation study between dual source CT perfusion imaging and the microvascular composition of solitary pulmonary nodules. *Lung Cancer*. 2019;130:115–20.
15. Ma SH, Xu K, Xiao ZW, Wu M, Sun ZY, Wang ZX, et al. Peripheral lung cancer: relationship between multi-slice spiral CT perfusion imaging and tumor angiogenesis and cyclin D1 expression. *Clin Imaging*. 2007;31:165–77.
16. Miles KA, Charnsangavej C, Lee FT, Fishman EK, Horton K, Lee TY. Application of CT in the investigation of angiogenesis in oncology. *Acad Radiol*. 2000;7:840–50.
17. Tacelli N, Remy-Jardin M, Copin MC, Scherpereel A, Mensier E, Jaillard S, et al. Assessment of non-small cell lung cancer perfusion: pathologic-CT correlation in 15 patients. *Radiology*. 2010;257:863–71.
18. Ippolito D, Sironi S, Pozzi M, Antolini L, Ratti L, Meloni F, et al. Perfusion computed tomographic assessment of early hepatocellular carcinoma in cirrhotic liver disease: initial observations. *J Comput Assist Tomogr*. 2008;32:855–8.
19. Larke FJ, Kruger RL, Cagnon CH, Flynn MJ, MN MN-G, Wu X, et al. Estimated radiation dose associated with low-dose chest CT of average-size participants in the National Lung Screening Trial. *Am J Roentgenol*. 2011;197:1165–9.
20. Chae EJ, Song JW, Krauss B, Song KS, Lee CW, Lee HJ, et al. Dual-energy computed tomography characterization of solitary pulmonary nodules. *J Thorac Imaging*. 2010;25:301–10.
21. Reiter MJ, Winkler WT, Kagy KE, Schwoppe RB, Lisanti CJ. Dual-energy computed tomography for the evaluation of enhancement of pulmonary nodules ≤ 3 cm in size. *J Thorac Imaging*. 2017;32:189–97.
22. Chae EJ, Song JW, Seo JB, Krauss B, Jang YM, Song KS. Clinical utility of dual-energy CT in the evaluation of solitary pulmonary nodules: initial experience. *Radiology*. 2008;249:671–81.
23. Chen L, Zhang J, Bao J, Zhang L, Hu X, Xia Y, et al. Meta-analysis of diffusion-weighted MRI in the differential diagnosis of lung lesions. *J Magn Reson Imaging*. 2013;37:1351–8.
24. Ruilong Z, Daohai X, Li G, Xiaohong W, Chunjie W, Lei T. Diagnostic value of 18F-FDG-PET/CT for the evaluation of solitary pulmonary nodules: a systematic review and meta-analysis. *Nucl Med Commun*. 2017;38:67–75.
25. Li S, Zhao B, Wang X, Yu J, Yan S, Lv C, et al. Overestimated value of (18)F-FDG PET/CT to diagnose pulmonary nodules: analysis of 298 patients. *Clin Radiol*. 2014;69:e352–7.

How to cite this article: Zhu B, Zheng S, Jiang T, Hu B. Evaluation of dual-energy and perfusion CT parameters for diagnosing solitary pulmonary nodules. *Thorac Cancer*. 2021;12:2691–7. <https://doi.org/10.1111/1759-7714.14105>